THE JOURNAL OF BIOLOGICAL CHEMISTRY
Vol. 272, No. 4, Issue of January 24, pp. 2060–2068, 1997
Printed in U.S.A.

Random Mutagenesis of the cAMP Chemoattractant Receptor, cAR1, of *Dictyostelium*

MUTANT CLASSES THAT CAUSE DISCRETE SHIFTS IN AGONIST AFFINITY AND LOCK THE RECEPTOR IN A NOVEL ACTIVATIONAL INTERMEDIATE*

(Received for publication, August 16, 1996, and in revised form, October 21, 1996)

Ji-Yun Kim‡, Michael J. Caterina‡§, Jacqueline L. S. Milne¶, Kenneth C. Lin, Jane A. Borleis, and Peter N. Devreotes‖

From the Department of Biological Chemistry, The Johns Hopkins University, School of Medicine, Baltimore, Maryland 21205

The cAMP chemoattractant receptor, cAR1, of *Dictyostelium* transduces extracellular cAMP signals via G protein-dependent and G protein-independent mechanisms. While site-directed mutagenesis studies of G protein-coupled receptors have provided a host of information regarding the domains essential for various functions, many mechanistic and structural questions remain to be resolved. We therefore carried out polymerase chain reaction-mediated random mutagenesis over a large part of the cAR1 sequence (from TMIII through the proximal part of the cytoplasmic tail). We devised a rapid screen for loss-of-function mutations based on the essential role of cAR1 in the developmental program of *Dictyostelium*. Although there were an average of two amino acid substitutions per receptor, ~90% of the mutants were able to substitute for wild-type cAR1 when expressed in receptor null cells. About 2% were loss-of-function mutants that expressed wild-type levels of receptor protein. We used biochemical screens to select about 100 of these mutants and chose eight representative mutants for extensive characterization. These fell into distinct classes. One class had a conditional defect in cAMP binding that was reversed by high salt. Another large class had decreased affinity under all conditions. Curiously, the decreases were clustered into three discrete intervals. One of the most interesting class of mutants lost all capacity for signal transduction but was phosphorylated in response to agonist binding. This latter finding suggests that there are at least two activated states of cAR1 that can be recognized by different downstream effectors.

G protein[1]-coupled receptors (GPCR) constitute a large and diverse family of molecules that span the plasma membrane seven times and transduce extracellular signals using heterotrimeric G proteins (1, 2). Ligands for this family of receptors vary from small compounds like cAMP to large peptides (3–5). Despite the diversity of ligands, occupancy of these receptors typically triggers an analogous array of excitation and desensitization events (6). The occupied receptors activate heterotrimeric G proteins which, in turn, activate downstream effector molecules, such as adenylyl cyclases, ion channels, phosphodiesterases, and phospholipases (7, 8), and also mediate additional changes that do not require heterotrimeric G proteins (9). These include changes in plasma membrane ion permeability (10) and gene expression as well as processes that attenuate the receptor's ability to bind ligands and transduce signals (11–13).

Site-directed mutagenesis and chimeric receptor studies have provided information regarding the interactions of GPCRs with G proteins, the localization of ligand contact sites, and the location of domains important for activational isomerization (14, 15). In the case of adrenergic receptors, catecholamines are thought to interact with amino acid residues within a pocket formed by the transmembrane helices. The domains important in coupling to G proteins reside in small segments exiting from TMV, TMVI, and TMVII to the cytoplasmic loops (16, 17). Segments of the third intracellular loop, in particular, determine the specificity of G protein coupling (18, 19). From these studies, a general model has emerged; agonist binding rearranges interactions among the helices and transmits conformational changes to the segments exiting from membrane to cytoplasm (20). These changes are then detected by intracellular components of the signaling machinery. Despite these advances, much remains to be learned about the molecular determinants for ligand binding to G protein-coupled receptors and the sequence of events that follow.

We devised a genetic screen to isolate random mutations that alter the biological and biochemical properties of the chemoattractant receptors of *Dictyostelium*. This organism utilizes four homologous receptors (cAR1–cAR4), which vary in affinity for cAMP, to coordinate morphological transitions throughout a developmental program in which individual amoebae aggregate to form multicellular structures (21, 22). Cells clonally seeded on bacterial lawns divide and, by consuming the bacteria, create plaques. Within several days, the cells in the centers of these plaques are induced by starvation to aggregate and form macroscopic fruiting bodies (23). Cells lacking cAR1 or expressing only defective versions of the receptor fail to aggre-

* This work is supported in part by National Institutes of Health Grant GM 34933 (to P. N. D.). The costs of publication of this article were defrayed in part by the payment of page charges. This article must therefore be hereby marked "*advertisement*" in accordance with 18 U.S.C. Section 1734 solely to indicate this fact.

‡ These two authors contributed equally to this work.

§ Supported by a National Institutes of Health Medical Student Training Program Grant. Current address: Dept. of Cellular and Molecular Pharmacology, University of California, San Francisco, San Francisco, CA 94143.

¶ Recipient of a Centennial Fellowship from the Medical Research Council of Canada.

‖ To whom all correspondence should be addressed: Dept. of Biological Chemistry, The Johns Hopkins University, School of Medicine, 725 N. Wolfe St., Baltimore, MD 21205. Tel.: 410-955-4699; Fax: 410-955-5759.

[1] The abbreviations used are: G protein, guanine nucleotide-binding regulatory protein; GPCR, G protein-coupled receptor; cAR1, cAMP receptor; TM, transmembrane; PCR, polymerase chain reaction; Pipes, 1,4-piperazinediethanesulfonic acid; PAGE, polyacrylamide gel electrophoresis; DB, development buffer.

gate or differentiate (24) and therefore form smooth plaques, providing a convenient biological "read out" for function. This screen has allowed us to rapidly assess thousands of point mutations in the receptor and identify those affecting particular functions.

At the outset, we expected to find mutants which failed to bind cAMP or were defective in coupling to G proteins or G protein-independent pathways. We found that most amino acid substitutions did not impair receptor function. Of those that did, we saw a large array of phenotypes that fell into multiple classes. In some mutants, the cAMP binding affinity was decreased conditionally at low ionic strength or, alternatively, decreased under all conditions to one of three discrete steps. In other mutants, cAMP binding and agonist-induced phosphorylation were intact, but signaling through G protein-dependent and G protein-independent pathways was defective. These mutant classes complement those of a companion study (50), which describes a series of mutants derived from random mutagenesis of the third intracellular loop.

MATERIALS AND METHODS

PCR Mutagenesis and Mutant Library Construction—The 1.3-kilobase pair cAR1 cDNA, *Eco*RI-*Eco*RI fragment, was subcloned into the *Eco*RI site of pPL1 (25) in *Bgl*II (5′-end)-*Bam*HI (3′-end) orientation to construct pJK53. This plasmid was used as a template for PCR under conditions designed to induce frequent misincorporation of nucleotides (26). Briefly, 1 ng of pJK53 PCR-template was incubated with 30 ng each of primers T3 and T7, 1 mM each of dCTP, dGTP, and dTTP, 0.2 mM dATP, 7 mM $MgCl_2$, 0.5 mM $MnCl_2$, and 5 units *Taq* thermostable DNA polymerase (Perkin-Elmer) in 10 mM Tris, pH 8.3, in a final volume of 100 μl. The reaction was carried out in a thermal cycler (Perkin-Elmer) for 30 cycles with 94 °C, 1.5-min denaturation, 45 °C, 2-min annealing, and 72 °C, 2-min extension. The resulting PCR products were extracted with phenol-chloroform, then digested simultaneously with *Bam*HI, *Nde*I, and *Bst*XI. The mutagenized *Nde*I/*Bst*XI fragment (583 base pairs), encoding the amino acids from the third to the seventh cAR1 transmembrane domains, was gel-purified and used to replace the corresponding wild-type *Nde*I/*Bst*XI fragment of pJK53. The resulting mutant cAR1 cDNAs were excised with *Bam*HI/*Bst*XI and directionally subcloned into *Dictyostelium* expression vector, pMC34 (27).

Transformation and Cell Culture—Transformation of the mutant cAR1 library into *car1*$^-$ or *car1*$^-$/*car3*$^-$ cells was performed by electroporation as described previously (27). One day after electroporation, nonselective medium was replaced with HL-5 containing G418 (Geneticin) (20 μg/ml), and for each transformation, 4×10^6 cells were placed into each well of a 24-well plate. For the initial aggregation assay, approximately 150 *Dictyostelium* clones from each of the 24 wells were seeded onto SM agar plates with lawn of *Klebsiella aerogenes*. After 5–6 days of growth and development, *Dictyostelium* plaques that created aggregation-deficient "smooth" plaques were picked into HL-5 with G418 (20 μg/ml). Plasmids DNA was recovered and transformed into bacteria as described (27). Bacterially propagated plasmids were then transformed by electroporation into *car1*$^-$/*car3*$^-$ or *car1*$^-$ cells for subsequent phenotypic analysis. The mutant plasmids were sequenced using automated sequencer.

Electrophoretic Mobility Shift Assay—The receptor electrophoretic mobility shift assay was performed as described elsewhere (28). Immunoblotting was performed using cAR1-specific rabbit polyclonal antiserum (29). Primary antibodies were detected using alkaline phosphatase-conjugated donkey anti-rabbit antibodies and chemiluminescence (Dupont).

DB Development Assay—Growth stage cells were washed once in development buffer (DB) (30), and 10 million cells were plated onto a 35-mm 1% DB agar plates and allowed to settle for 20 min. Excess buffer was drained, and cells were left undisturbed for 24 h at 22 °C to undergo development (30).

Adenylyl Cyclase Assay—Cells grown in shaking culture were washed with DB, developed with 300 nM cAMP pulses every 6 min for 6 h, and shaken rapidly for 30 min in the presence of 5 mM caffeine to inhibit the cAMP oscillation and to obtain cells with basal level of adenylyl cyclase activity (31). After basalation, cells were washed 4 times with ice-cold phosphate manganese buffer (10 mM KH_2PO_4, pH 6.5, 2 mM $MgSO_4$) to remove caffeine, resuspended to 8×10^7 cells/ml, and kept on ice until use. Cells were transferred to 22 °C, stimulated with 10^{-3} M cAMP at time 0, and the amount of [α-^{32}P]ATP converted into [^{32}P]cAMP in 1 min was measured as described previously (32).

Actin Polymerization Assay—Cells were developed as in the adenylyl cyclase assay, resuspended in phosphate manganese buffer (see above), and placed on ice. Ten minutes before each experiment, cells were transferred to a rotary shaker (200 rpm) at 22 °C. At time 0, 10^{-7} M cAMP and 10 mM dithiothreitol were added to induce actin polymerization, and at various times, the reactions were stopped by transferring the aliquots of cells into fixing solution (3.7% formaldehyde, 10 mM Pipes, 0.1% Trion X-100, 20 mM K_2HPO_4, 5 mM EGTA, 2 mM $MgCl_2$, and 250 nM tetramethylrhodamine B isothiocyanate-phalloidin, pH 6.8) (33). After staining at least 1 h at room temperature, fixed cells were pelleted in a tabletop centrifuge (14,000 rpm, 5 min), and the pellet was resuspended into 1 ml of methanol. Rhodamine fluorescence was detected with a Perkin-Elmer fluorescence spectrophotometer (excitation at 540 nm, emission at 575 nm).

cAMP Binding—cAMP binding assays were performed in either phosphate buffer or in the presence of 3 M ammonium sulfate as described previously (11). Scatchard data were analyzed using the software program LIGAND.

GTP Inhibition of Binding—Cells were developed as before, washed once in phosphate buffer, and resuspended to 6×10^7/ml. Cell were then lysed through 5-μm filters (Millipore), and the lysates were pelleted (5 min, 10,000 rpm SS34 rotor). The membrane pellets were washed once and resuspended in phosphate buffer to a density of 8×10^7 cell equivalent/ml and kept on ice. The amount of cAMP binding to membrane measured with 2 nM [^{3}H]cAMP either in the presence or absence of 100 μM GTP was then assessed by spinning the membrane through silicon oil as described previously (34).

Ca^{2+} Influx Assay—$^{45}Ca^{2+}$ entry was followed for 40 s in the presence or absence of cAMP using a standard centrifugation assay. Values shown are the ratio of Ca^{2+} uptake into cAMP-treated cells/Ca^{2+} uptake into unstimulated cells (35).

Site-directed Mutagenesis—Oligonucleotide-directed mutagenesis of cAR1 was performed in bacteriophage M13 as described elsewhere (27) to create cDNAs encoding mutants I-22 and II-22. The resulting cDNAs were subcloned into pMC34 (27).

RESULTS

Mutant Library Construction, Expression, and Initial Biological Screen—We used PCR under conditions of decreased fidelity to generate a population of mutant cAR1 cDNAs (26). Each receptor contained an average of two amino acid substitutions within the region extending from within the third transmembrane domain to the proximal portion of the cytoplasmic carboxyl terminus (residues 88–264). Over 2000 mutant cDNAs were subcloned into a segregating extrachromosomal plasmid that direct expression of the receptor throughout growth and early development (27). The plasmid library was electroporated into *car1*$^-$ cells (28), and about 4000 transformants were allowed to form plaques on bacterial lawns for phenotypic screening and subsequent characterization (Fig. 1).

The results of a typical mutant screen are illustrated in Table IA. Of 1659 transformants analyzed, nearly 90% regained fully the ability to aggregate. Of the remaining 193 clones, 177 exhibited very weak aggregation, and 16 were completely aggregation-deficient. An aggregation-deficient phenotype could result from the expression of a dysfunctional cAR1 mutant or, alternatively, from low receptor protein expression. To distinguish these possibilities, we immunoblotted 116 non-aggregating or weakly aggregating clones for cAR1 expression. About two-thirds of the clones had little or no cAR1, while the remainder had wild-type levels of the protein (Table IB). We focused our studies on the latter type of clones isolated from four independent transformations and screens.

Initial Biochemical Characterization—We carried out several tests to define the biochemical basis of the aggregation-deficient phenotype conferred by these mutant receptors. The initial test examined agonist-induced phosphorylation. Upon cAMP binding, serine residues (Ser-303 and Ser-304) in the carboxyl-terminal cytoplasmic domain of cAR1 undergo phosphorylation, resulting in a discrete mobility retardation on

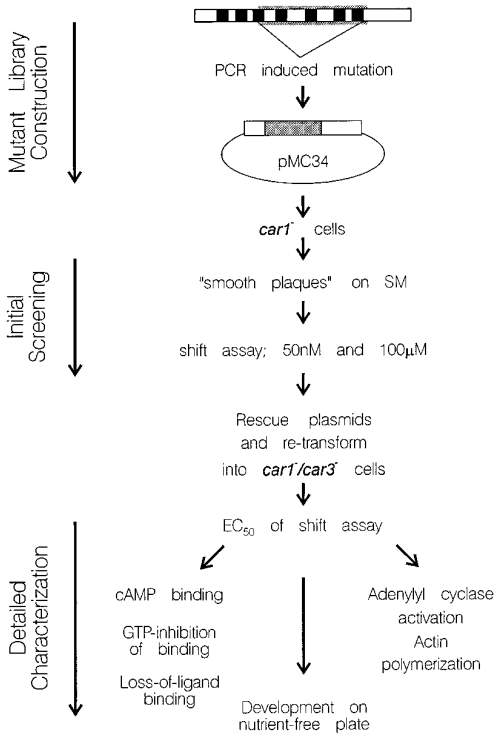

FIG. 1. **PCR-mediated random mutagenesis and screening strategy.** A flow diagram of the random mutagenesis and screening strategy is shown. At the top is a schematic topological representation of cAR1 with transmembrane domains shown as *filled bars*. The region mutagenized is shown as a *shaded area*, from residue 88 (middle of TMIII) to the residue 264 (distal end of TMVII adjacent to the cytoplasm). Initial characterization of the pool of mutant receptors was carried out in a *car1*$^-$ cell line. Plasmid-encoding specific mutants were rescued and retransformed into *car1*$^-$/*car3*$^-$ cells for further characterization (see text for details).

SDS-PAGE (11, 36). This alteration, detected by immunoblot, provides a convenient method for assessing agonist activated receptor-kinase coupling. At steady-state, the fraction of receptors in the slower mobility form is proportional to the concentration of the applied stimulus (37). When the assay is carried out at multiple concentrations of cAMP, the EC_{50} typically reflects the cAMP binding affinity (38).

In our initial screen, we treated the mutant expressing clones with three concentrations of cAMP, 0, 50 nM, and 100 μM for 15 min, sufficiently long to attain the steady state. Since the EC_{50} is 35 nM (Fig. 2), at 50 nM the majority of wild-type cAR1 molecules are found in the slower mobility form. At 100 μM, even very low affinity receptors are expected to be maximally occupied and phosphorylated (28). When 93 clones treated with cAMP at these three concentrations were examined, the mutants fell into five categories based on the severity of the impairment (Table II). Eighteen of the clones (19.4%) exhibited a profile identical to that seen with wild-type cAR1 (row a); the remaining 75 exhibited an altered profile. Of these, 60 (64.5%) responded fully to 100 μM but displayed only a partial or no response to 50 nM (rows b and c). The remaining 15 (16.1%) exhibited little or no response even at 100 μM (rows d and e).

We carried out additional assays to further classify the mutants. We measured binding of [^{3}H]cAMP to intact cells in phosphate buffer at 16 nM and in ammonium sulfate at 25 nM. Since the K_d of cAR1 under physiological conditions in phosphate buffer is 25–300 nM, the former assay is designed to quickly distinguish high from low affinity receptors. The ammonium sulfate assay is designed to measure the total number of binding sites, since addition of the salt reduces the K_d of wild-type cAR1 to about 8 nM (39). The cAMP-induced electrophoretic mobility shift profiles of the mutants corresponded with the amount of [^{3}H]cAMP bound under physiological conditions. The amount of binding measured in the presence of ammonium sulfate also paralleled these data (data not shown).

TABLE I
Typical distribution of mutant phenotypes in an initial screen of the cAR1 mutant library

1659 independent transformants were spread clonally on *K. aerogenes* lawns and allowed to form plaques. The formation of macroscopic multicellular aggregates was then assayed by visual inspection, with the assistance of a dissecting microscope. Values shown represent the number and percentage of clones exhibiting each phenotype (A). Of those clones exhibiting weak aggregation or no aggregation, 116 were assessed for cAR1 expression by dot immunoblotting as described under "*Materials and Methods*" (B).

	Assay	No. of clones	Percent of total
			%
A.	Strong aggregation	1466	88.5
	Weak aggregation	177	10.6
	No aggregation	16	0.9
	Total clones screened	1659	100.0
B.	cAR1	37	31.8
	No or little cAR1	79	68.2
	Total screened	116	100.0

We rescued the plasmids encoding eight representative mutants, one from row a, three from the row d, and two from the rest to represent the biochemical phenotypes observed in the initial screen (Table II), retransformed them into *car1*$^-$ or *car1*$^-$/*car3*$^-$ cells, and subjected them to more extensive characterization. With the exception of the cAMP-induced electrophoretic mobility shift experiments which were carried out in a *car1*$^-$ background, all of the following studies were carried out in a *car1*$^-$/*car3*$^-$ background. We chose these backgrounds for the following reason. Although the *car1*$^-$ cells do not aggregate upon starvation and therefore are adequate for initial identification of functionally deficient receptors, some of the cAMP-mediated responses still persist in the *car1*$^-$ cells (40, 41). On the other hand, in the *car1*$^-$/*car3*$^-$ cell, cAMP responsiveness is completely absent (41), and expression of wild-type cAR1 restores all of the measured wild-type functions.

cAMP-induced cAR1 Phosphorylation—We next examined the full concentration dependence of the cAMP-induced electrophoretic mobility shift of the eight representative mutants (Fig. 2). On the basis of these dose-response profiles and the cAMP binding analysis presented below, the eight mutants fell into the following classes, I, II, and IIIa–c. For wild-type cAR1, the EC_{50} was 35 nM, consistent with our previously published results (28, 38). Mutant I-21 exhibited a nearly wild-type concentration-dependence, while mutants IIIa-21 and IIIa-22 and IIIb-21 and IIIb-22 required about 5 and 100 times higher cAMP concentrations, respectively (Fig. 2). The two class IIIc mutants failed to show a mobility shift, even at the highest cAMP concentrations (10^{-2} M) tested. The electrophoretic mobility shift of three additional mutants (IIIa-23, IIIb-23, and IIIc-23) also exhibited EC_{50} increases clustered around these 5-fold, 100-fold, and infinite ranges (data not shown). Mutant II-21 displayed a dose dependence similar to that of the class IIIb mutants; however, it was placed in a separate class because of its unique binding properties, as described below. For these 11 mutants, the full cAMP concentration dependence of this response was consistent with that observed in the rapid two-dose screening assay (Table II). Therefore the electrophoretic mobility shift phenotypes exhibited in the initial screen, although crude, represented intrinsic, reproducible properties of the mutants, and Fig. 2 and Table II reflect the distribution of observable phenotypes.

Rescue of the car1$^-$/*car3*$^-$ *Developmental Phenotype*—We

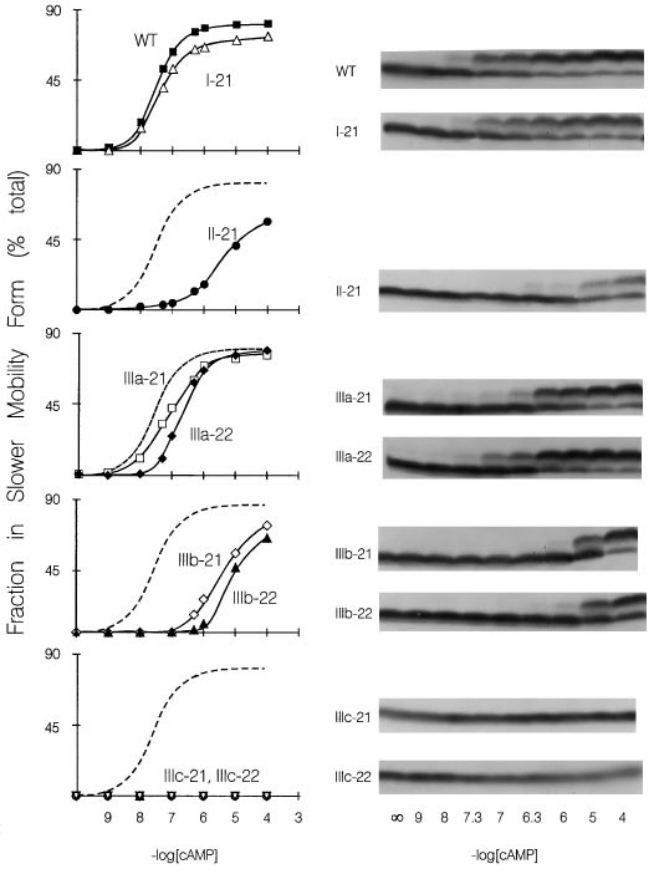

FIG. 2. **cAMP concentration dependence of phosphorylation of selected cAR1 mutants.** *car1*$^-$ cells were transformed with a plasmid encoding wild-type cAR1 (*top panel*, *filled squares*) or one of the eight receptor mutants shown. Growth stage cells were washed with phosphate buffer and incubated with cAMP (0, 1 nM, 10 nM, 50 nM, 100 nM, 500 nM, 1 μM, 10 μM, or 100 μM) for 15 min in the presence of 10 mM dithiothreitol and 5 mM caffeine. Cells were lysed in sample buffer, subjected to SDS-PAGE, and immunoblotted for cAR1. The resulting autoradiographs were then scanned and quantitated to generate the curves shown on the *left*. Values are shown as the fraction of receptor in the lower mobility form and represent the means of at least two independent experiments. A representative autoradiograph for each mutant is shown on the *right*.

next carried out a more extensive phenotypic analysis of the eight mutants. Exponentially growing cells were washed and spread on nutrient-free agar plates. Under these conditions, cells expressing wild-type cAR1 aggregate and form fruiting bodies within 24–48 h, while the vector-transformed cells remain as a monolayer (Fig. 3, *A* and *B*). The results for one member of each class are illustrated in Fig. 3, *C–G*. The members of classes I, II, and IIIc failed to restore any sign of aggregation (Fig. 3, *C*, *D*, and *G*), while the members of the remaining two subclasses, IIIa and IIIb, mediated aggregation to varying degrees. Cells expressing either of the two IIIa mutants nearly always aggregated and were capable of forming slugs and fruiting bodies with a relatively wild-type morphology (Fig. 3*E*). Cells expressing either of the two IIIb receptors could also aggregate, although a smaller fraction of cells participated. These formed either loose mounds that went on to form tiny fruiting bodies (Fig. 3*F*) or tight aggregates that transformed into normal fruiting bodies. Thus, among the class III subclasses, there is a correlation between the efficacy of the expressed receptor and the resulting aggregation phenotype.

cAMP Binding Analysis—We next measured the affinity of [^{3}H]cAMP binding to the mutant receptors. Since the members of a given class displayed similar properties, we chose one from each of the classes for detailed binding analysis (I-21, II-21, IIIa-21, IIIb-21, and IIIc-21). The resulting Scatchard data are illustrated in Fig. 4 and Table III. Wild-type cAR1 displayed two classes of binding sites as described previously. Most (about 93%) of the sites had an affinity of 500 nM, while a small fraction had an affinity of 30 nM in phosphate buffer. Since the lower affinity sites constitute most of the binding sites, we concentrated our analysis on them. As shown in Fig. 4*A*, the affinities of the class III mutants, measured in phosphate buffer, corresponded to the relative EC_{50} values of their electrophoretic mobility shift. IIIa-21 had a 5–7-fold lower cAMP sensitivity than wild-type cAR1, as assessed by both EC_{50} and K_d; IIIb-21 had a >10-fold decreased sensitivity reaching the detection limit of the binding assay; and IIIc-21 did not show any detectable cAMP binding (data not shown). The affinities of the class III mutants, measured in ammonium sulfate, were also reduced in a corresponding pattern (Fig. 4*C*). The progressive decreases in cAMP efficacies and binding affinities are highly correlated for the class III mutants. The affinities and the EC_{50} of the electrophoretic mobility shift of subclasses IIIa, IIIb, and IIIc were moderate, low, and undetectable, respectively, as summarized in Table III.

TABLE II
Distribution of electrophoretic mobility shift profiles in functionally impaired cAR1 mutants

93 clones expressing mutant cAR1s at detectable levels but retaining an aggregation-deficient phenotype were treated with buffer alone (0), cAMP at 50 nM (low), or 100 μM (high) in the presence of 10 mM dithiothreitol and 5 mM caffeine for 15 min to reach steady state. Cells were lysed in sample buffer, subjected to SDS-PAGE, and immunoblotted for cAR1. The number and percentage of clones exhibiting each of the illustrated mobility shift profiles are listed. In this assay wild-type cAR1 exhibits the top most profile.

	Mobility Shift Pattern			Number of Clones	% of total
	0	50 nM	100 μM		
a	—	—	—	18	19.4
b	—	—	—	49	52.7
c	—	—	—	11	11.8
d	—	—	—	10	10.7
e	—	—	—	5	5.4

For mutant II-21, while the binding affinity of the receptor measured in phosphate buffer and estimated from the EC_{50} of the electrophoretic mobility shift was very similar to those of IIIa and IIIb mutants (Fig. 4*A*, Table III), its affinity measured in ammonium sulfate was as high as that of wild-type (Fig. 4*C*, Table III). This striking discrepancy between the two affinities is also observed for cAR2, the receptor expressed exclusively in the muticellular stages of development (42, 43).

For mutant I-21, the EC_{50} for the electrophoretic mobility shift was slightly higher than that of wild-type cAR1 (Fig. 2). Yet, its binding affinity measured in phosphate buffer was at least 5-fold greater than wild-type (Fig. 4*B*). This greater affinity of I-21 persisted when the binding was measured in ammonium sulfate (Fig. 4*D*, Table III).

Activation of Adenylyl Cyclase—To assess the coupling of the mutant receptors to G protein-mediated signaling pathways, we measured the capacity of each to mediate the activation of the adenylyl cyclase by extracellular cAMP (44). The cells were first induced to enter the developmental program and express the components of the adenylyl cyclase activation pathway. The expression of adenylyl cyclase was confirmed for each cell line

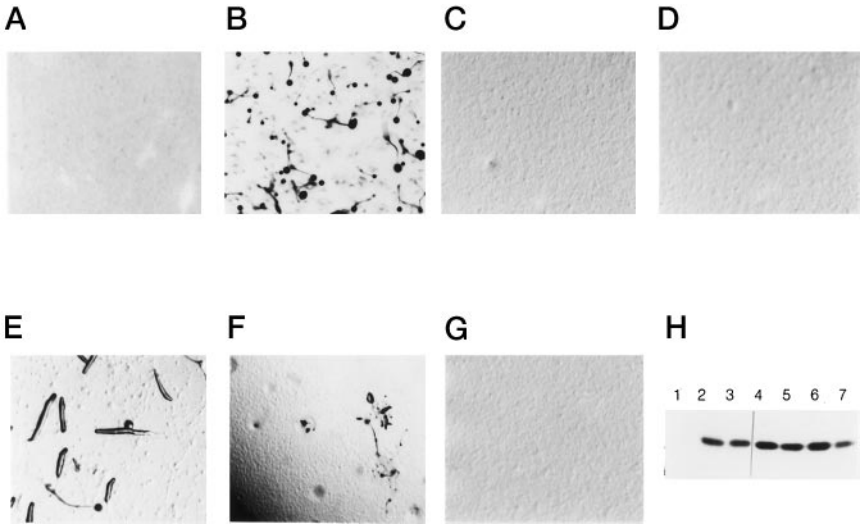

FIG. 3. **Rescue of the cAR1and cAR3 null aggregation-deficient phenotype by cAR1 mutants.** cAR1 and cAR3 double null cells (*car1*$^-$/*car3*$^-$) were transformed with control vector (*A*) or plasmids encoding wild-type cAR1 (*B*) or mutant I-21 (*C*), mutant II-21 (*D*), mutant IIIa-22 (*E*), mutant IIIb-21 (*F*), or mutant IIIc-21 (*G*). Growth stage cells were washed with DB, plated on non-nutrient DB agar plates, and incubated for 24–48 h at 22 °C. Magnification is 5× for *panels B*, *C*, *D*, *E*, and *G* and 12.5× for *panels A* and *F*. In parallel, an equivalent number of cells were lysed in sample buffer, subjected to SDS-PAGE, and immunoblotted with cAR1 antiserum to confirm the expression of mutant receptors (*H*). The order of the lanes corresponds to the order of the photographs, beginning at the *top*, *left*.

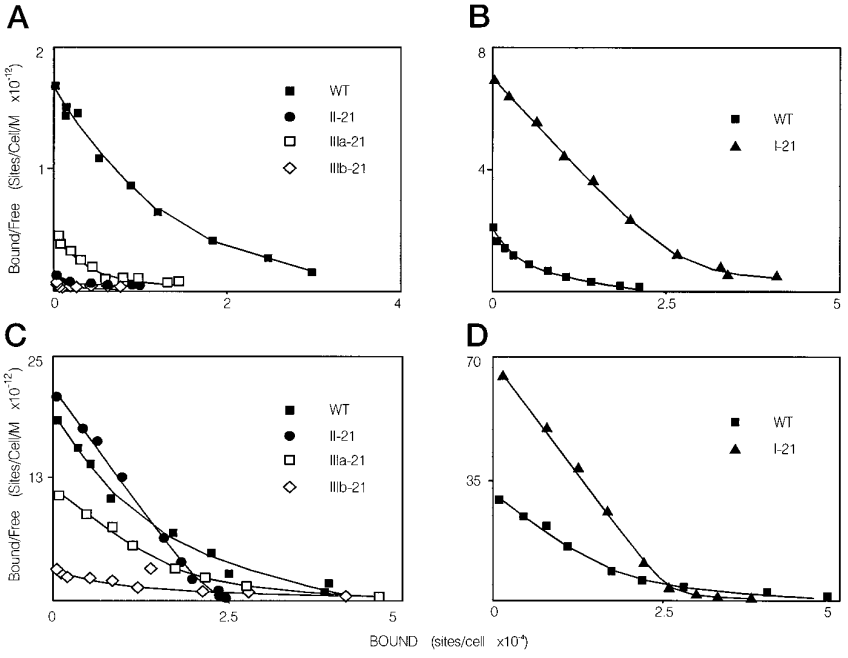

FIG. 4. **Scatchard analysis of [^{3}H]cAMP binding of the mutant receptors in phosphate buffer and ammonium sulfate.** cAMP binding was measured by competition of ^{3}H-labeled cAMP with unlabeled cAMP at cAMP concentrations ranging from 10^{-9} M to 2×10^{-6} M for phosphate buffer binding (*panels A* and *B*) and 10^{-10} M to 2×10^{-7} M for ammonium sulfate (*panels C* and *D*) binding on growth stage cells overexpressing wild-type or mutant receptors. Bound cAMP was separated from unbound cAMP by sedimenting the cells through silicon oil in the case of phosphate buffer binding or washing once with 3 M ammonium sulfate in the ammonium sulfate binding analysis. Data represent the means of triplicate determinations from one of at least two separate experiments. The *line* connecting data points was generated by the fitting program, LIGAND (see "Materials and Methods").

by immunoblot (Fig. 5*B*). Intact cells were then stimulated with a sufficiently high concentration of cAMP (10^{-3} M) to saturate the binding sites of even the lowest affinity receptors. We verified the activation of each mutant receptor by demonstrating that the expressed receptors shifted to the slower electrophoretic mobility form after cAMP stimulation. The *car1*$^-$/*car3*$^-$ cells transformed with empty vector exhibited no measurable activation of adenylyl cyclase (Fig. 5*A*), while those expressing wild-type cAR1 exhibited a rapid, transient rise in activity. The mutant receptors capable of restoring aggregation competence (IIIa-21 and IIIb-21) mediated an essentially wild-type adenylyl cyclase response. In contrast, mutants I-21 and II-21 failed to activate adenylyl cyclase. This observation offers an explanation for the complete inability of these two mutants to restore aggregation competence (Fig. 3, *C* and *D*). It also suggests that mutants I-21 and II-21 are impaired in G protein activation despite the fact that they bind cAMP and display agonist-induced phosphorylation.

Actin Polymerization Assay—As a second method to assess the ability of each mutant receptor to activate G protein-dependent signaling pathways, we monitored cAMP-stimulated actin polymerization (45). The actin polymerization assays and the adenylyl cyclase assays described above were performed in parallel as to allow a reliable comparison between the results. When the stimulus was applied, a rapid and transient increase in F-actin was observed in cells transformed with wild-type cAR1; vector control transformants showed no response (Fig. 5*C*). The mutants that restored aggregation (IIIa-21, IIIb-21) responded fully, while those that did not rescue the phenotype (I-21 and II-21) showed no agonist-induced F-actin response.

Separation of Two Mutations in Mutant II-21—As noted above, mutant II-21 displayed very low affinity in phosphate buffer but high affinity in ammonium sulfate, which is reminiscent of cAR2. Unlike cAR2, however, which can activate cAMP-mediated adenylyl cyclase and actin polymerization (reviewed in Kim *et al.* (46)), II-21 did not transduce either signals (Fig. 5, *A* and *C*). Sequence analysis revealed that II-21 had two substitutions (R160S and H191P) in the second extracellular loop and in the third intracellular loop, respectively (Fig. 6*A*). We separated these two mutations by site-directed mutagenesis. The resulting mutants split the phenotype of II-21. H191P failed to transduce signals but displayed higher affinity than cAR1 (Fig. 6, *C* and *D*) and therefore was classified as I-22; R160S retained the binding characteristics of the original II-21

TABLE III

Summary of cAMP binding affinity in phosphate buffer and ammonium sulfate and EC_{50} of electrophoretic mobility-shift of mutants

Data from two independent cAMP binding experiment illustrated in Fig. 4 and other experiments were subjected to computer fitting analysis using the program LIGAND. [^{3}H]cAMP binding was determined at 10 different cAMP concentrations ranging from 1×10^{-9} to 2×10^{-6} M in phosphate buffer (PB) or 1×10^{-10} to 2×10^{-7} M in the presence of 3 M ammonium sulfate (AS). The K_d (nM) and B_{max} (sites/cell $\times 10^{-3}$) values are means ± SE of one experiment performed in triplicate. One representative result from each mutant class that statistically fits data the best is shown. The B_{max} of a given cell line varied from day to day of experiments but was consistently within the ranges of 3×10^5 to 5×10^5 sites/cell. The relative proportion of the high and low affinity sites are normalized to the total number of sites/cell and presented as the percent of total. The EC_{50} values of the electrophoretic mobility shift were obtained by quantitatively scanning the immunoblots shown in Fig. 2.

Mutant class		K_d in PB		K_d in AS		EC_{50}	Relative EC_{50}
		Site 1	Site 2	Site 1	Site 2		
						nM	
Wild-type	K_d	34 ± 13	517 ± 131	2 ± 1	36 ± 11		
	% of B_{total}	7	93	23	77	35	1
I-21	K_d	20 ± 13	123 ± 40	1 ± 0.1	8 ± 5		
	% of B_{total}	8	92	20	80	50	1.2
I-22	K_d	38 ± 13	254 ± 104	6 ± 1			
(H191P)	% of B_{total}	88	12	100		50	1.2
II-21	K_d		4237 ± 487	5 ± 0.4	124 ± 82		
	% of B_{total}		100	84	16	5000	120
II-22	K_d		5128 ± 782	3 ± 0	197 ± 16		
(R160S)	% of B_{total}		100	61	39	500	12
IIIa-21	K_d	4 ± 1	3664 ± 559	2 ± 0.3	156 ± 43		
	% of B_{total}	2	98	6	94	250	7
IIIb-21	K_d		7407 ± 2628	16 ± 4	348 ± 122		
	% of B_{total}		100	11	89	5000	120
IIIc-21	NA		∞		∞	∞	∞

mutant but effectively transduced signals (Fig. 6, *C* and *D*, and Table IV) and was thus classified as II-22. The cAMP binding affinities of mutant I-22 measured in both phosphate buffer (38 and 250 nM) and ammonium sulfate (6 nM) were higher than wild-type (Fig. 6, *C* and *D*, and Table III). The EC_{50} of the electrophoretic mobility shift was similar to that of wild-type. I-22 failed to rescue development and only weakly activated adenylyl cyclase and actin polymerization (Table IV). For II-22, the EC_{50} of the electrophoretic mobility shift was 500 nM and the K_d in phosphate buffer was 5 μM; however, its affinity, measured in ammonium sulfate, was similar to wild-type (3 and 100 nM). This mutant was able to effectively activate adenylyl cyclase and rescue development (Table IV).

Mutant Sequence Analysis—To correlate the observed functional defects exhibited by these mutant receptors with the predicted structure of cAR1 (30), we sequenced each of the mutant cDNAs characterized in Table IV. The predicted topological positions of each of the amino acid substitutions observed for each mutant are illustrated in Fig. 7. Mutant I-21 has a single substitution, I108N, at the interface of TMIII and the second intracellular loop. The class III receptors have substitutions distributed throughout the mutagenized region. IIIa-21 possesses a single substitution, N210S, at the base of TMVI in the interface with the cytoplasmic loop. IIIa-22 has two substitutions, I171V and Y259H, at the base of the helices TMV and TMVII, respectively. IIIb-21 has a single substitution, N229D, that introduces a negatively charged residue into the proximal half of the third extracellular loop. IIIb-22 possesses 4 amino acid substitutions, L107S, F164Y, N197I, and I208Y, between the distal end of TMIII and the middle of TMVI. IIIc-21 has two substitutions, S90R and V189A, which introduce a positively charged residue at the top of helix TMIII and a conservative change in the third intracellular loop. IIIc-22 also contains two conservative substitutions, T97A and V136T, one in the middle of TMIII and another at the base of TMV.

DISCUSSION

In this study, we used random mutagenesis in conjunction with a biological screen and biochemical analyses to dissect the functions of a G protein-coupled receptor. We were thereby able to broadly survey the types of functional defects that mutations can create. An advantage of this approach over site-directed mutagenesis is the larger number of mutants that can be analyzed and the lack of bias in correlating mutations with expected defects. Nearly 2000 receptor mutants we screened possessed an average of two amino acid substitutions. Despite the extent of mutagenesis, nearly 90% of all mutants were able to rescue the aggregation-deficient phenotype of *car1*$^-$ cells. These mutant receptors must have been properly folded, transported to the plasma membrane, and deployed at the cell surface to display nearly wild-type properties of binding, signal transduction, and desensitization. Of the 12% of mutant receptors which failed to restore aggregation, or did so weakly, about one-third expressed wild-type levels of cAR1 protein. Using the cAMP-induced electrophoretic mobility shift of cAR1 as a rapid screen, we demonstrated that most of these mutants retained some extent of cAMP binding and receptor-kinase interaction. These findings suggest that there is a great range of substitutions within the cAR1 sequence that can be accommodated with little effect on functions. This supports and extends our previous observations on cAR1 third intracellular mutants and on a series of random chimeras between cAR1 and cAR2 (27, 28). Other investigators have reported that over 80% of randomly mutated G protein-coupled yeast pheromone receptors, bearing substitutions within their third intracellular loops, are capable of restoring pheromone responsiveness to receptor null cells (47).

On the basis of their biological and biochemical phenotypes, the mutants obtained in this study can be grouped into several classes. Class III mutants, which constitute the largest group obtained in our screen, are specifically defective in ligand binding affinity. Particularly intriguing is the fact that the cAMP sensitivities of these mutants, as assessed by cAMP binding

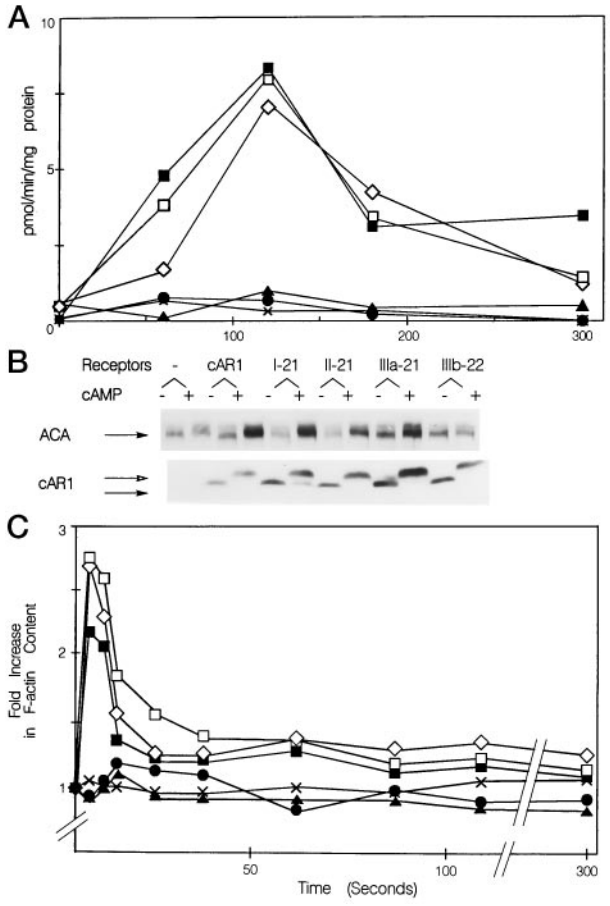

FIG. 5. **cAMP-mediated activation of adenylyl cyclase and actin-polymerization by mutant receptors.** *A*, using an "activation trap" assay, cAMP-induced adenylyl cyclase activity was performed as described under "Materials and Methods." *car1*$^-$/*car3*$^-$ cells expressing wild-type cAR1 or mutant receptors, or control vector clone was stimulated with 1 mM cAMP to assure saturation of all receptors, including low affinity mutants. At the indicated times aliquots of cells were rapidly lysed, and adenylyl cyclase activity was measured. *B*, aliquots of the cells before or after the cAMP addition for adenylyl cyclase assay were collected in the SDS-PAGE sample buffer, and the expression level and cAMP-induced electrophoretic mobility shift was measured by immunoblot with polyclonal antisera specific for either adenylyl cyclase or receptor. *C*, the same batch of developed cells was used to measure cAMP-induced actin polymerization. Since the EC_{50} of this response is lower that that of adenylyl cyclase activation (J. Borleis and P. N. Devreotes, unpublished results), cells were stimulated with 1 μM cAMP. At the indicated times, aliquots of cells were rapidly transferred to quenching solution in order to simultaneously stop the actin polymerization and stain filamentous actin with rhodamine-conjugated phalloidin. Vector control (×——×); wild-type cAR1 (■——■); mutant I-21 (▲——▲); mutant II-21 (●——●); mutant IIIa-21 (□——□); mutant IIIb-21 (◇——◇).

and the cAMP concentration dependence of receptor phosphorylation, were not distributed in a smooth continuum. Rather, these mutants fell into discrete subclasses, each possessing a narrow range of sensitivity with values of 250 nM (class IIIa), 5 μM (class IIIb), and infinity (class IIIc). This pattern of sensitivities raises the possibility that the deficits exhibited by class III mutants are modular; they might represent the selective disruption of one or more cAMP contact sites or, alternatively, of interactions of cAR1 with one or more cAR-associated proteins.

The IIIa mutants have conservative replacements in or at the base of the putative transmembrane helices. IIIa-22 contains a single substitution at the base of TMVI, while IIIa-21 contains two substitutions. Based on the importance of TMVII in receptor function shown in GPCRs, it is possible that the Y259H change at the base of TMVII is the residue that is responsible for the phenotype of this mutant receptor. IIIb-21 has a negatively charged residue in the distal portion of extracellular loop III, while IIIb-22 has four substitutions at four distinct regions and is difficult to interpret. Of the two substitutions in IIIc-21, the residue mutated within the third intracellular loop, V189, has been substituted with A, L, and F without significant effect in other studies (27, 50). The second mutation introduces a positively charged residue at the beginning of TMIII (S90R) and could have a more disruptive effect on receptor function. In contrast, the drastic phenotypic impairment of IIIc-21 is more difficult to understand since both substitutions are relatively conservative (T97A, V136T).

The class II mutants exhibit a markedly increased EC_{50} of electrophoretic mobility shift and a parallel reduction in cAMP binding affinity under physiological conditions. However, in the presence of 3 M ammonium sulfate, they have high affinity similar to cAR1 and thus have properties similar to those of wild-type cAR2, expressed during multicellular development (42, 43). These effects of ammonium sulfate on cAMP-binding are not fully understood. We have previously explored the cAMP binding properties of cAR2 by constructing a series of cAR1–cAR2 chimeras and mapping a domain of cAR1 which, when inserted into cAR2, conferred high affinity binding under physiological conditions. This domain is the carboxyl-terminal half of the second extracellular loop, which includes five amino acid differences between the two receptor subtypes (28). There are two extra negatively charged residues in cAR2, resulting in a net negative charge, compared to a net positive charge in cAR1 (48). Based on these observations, we proposed that the second extracellular loop plays an unique role in modulating ligand binding. In this study we found that the removal of a positive charge (R160S) in the same domain results in a similar conditional reduction of affinity. Thus, the changes in the net charge of the second extracellular loop appears to modulate access to an "intrinsic" binding site and thereby lower the apparent affinity, in effect acting as a "gatekeeper" region rather than as an actual contact site. As mentioned earlier, mutant IIIb-21 has a substitution, N229D, that results in a net charge reduction in the third extracellular loop. Unlike class II mutants, however, IIIb-21 exhibited reduced binding affinities in both phosphate buffer and high salt assays. Thus, the conditional "gatekeeper" function we propose is very specific to the second extracellular loop.

The mutants I-21 (I108N) and I-22 (H191P) comprise a novel and interesting class. These mutants are completely incapable of restoring aggregation to *car1*$^-$/*car3*$^-$ cells. This deficiency cannot be explained by impaired cAMP binding (the affinities of these receptors actually exceed that of wild-type receptor) or by defects in agonist-induced phosphorylation, which was barely affected. More likely, the inability of these mutants to restore aggregation is due to their failure to mediate signal transduction responses including, adenylyl cyclase, actin polymerization, and Ca^{2+} influx. The first two of these deficits suggest an impairment in G protein activation. As with other GPCRs, the ligand binding affinity of cAR1 is modulated by G protein interaction. The exceptionally high cAMP binding affinity of the class I mutants and its insensitivity to exogenously supplied GTP to reduce that affinity (Table IV) suggest that they may be able to associate with but unable to activate and release heterotrimeric G proteins. A similar mutant of rhodopsin locked in association with the GDP-bound form of transducin has been described (49).

Why do these mutant receptors fail to carry out certain G protein-independent responses such as ligand-induced Ca^{2+} influx? If they are locked in a nonproductive complex with

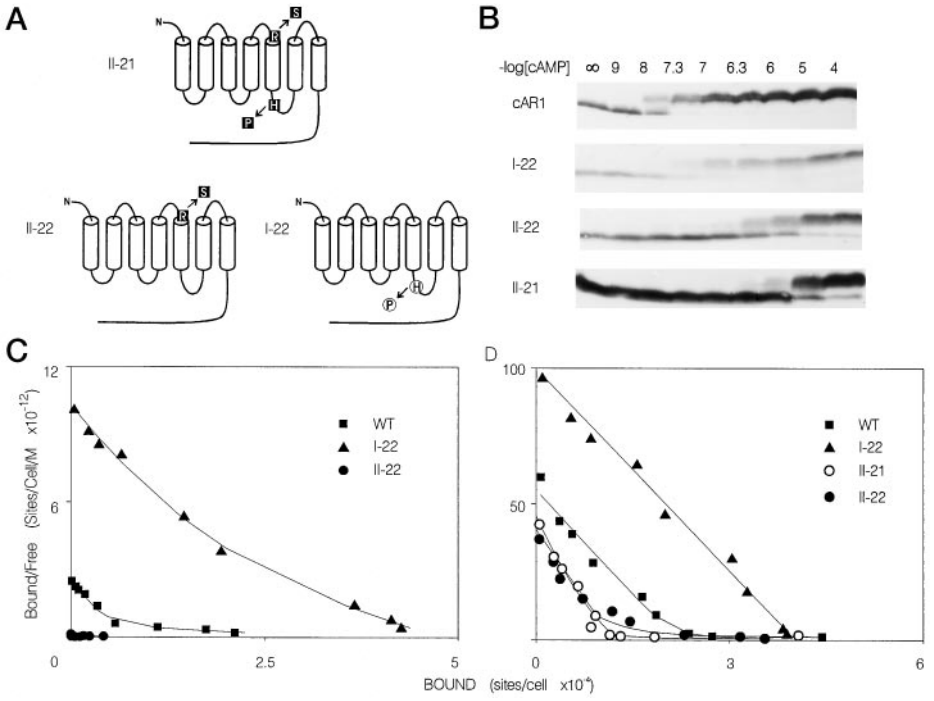

FIG. 6. **Characterization and reclassification of mutants I-22 (H191P) and II-22 (R160S).** *A*, schematic diagram of the two substitutions sustained by mutant II-21. The single substitution mutants (R160S and H191P) generated by site-directed mutagenesis are also shown. Single letter designation of amino acid shown on the putative topological structure of cAR1 is wild-type sequence and the residues these are changed to in each of the mutants are shown outside of the protein structure. *B*, agonist-induced electrophoretic mobility shift for cAR1, II-21, II-22 (R160S), and I-22 (H191P) at varying doses of cAMP is shown. *C* and *D*, binding characteristics of II-21 and new mutants, I-22 and II-22, both in phosphate buffer (*panel C*) and in ammonium sulfate (*panel D*). The measurements and analysis were done as described previously in Fig. 4. LIGAND-generated parameters are summarized in Table III.

TABLE IV
Summary of the mutant phenotypes

Various biochemical phenotypes of the mutants are summarized. Aggregation was assessed as shown in Fig. 3. (+++) indicates "wild-type like" phenotype with most cells participating in aggregation to form phenotypically normal fruiting bodies. (+) indicates either less efficient aggregation or aggregation only at high cell densities. (−) indicates that all attempts at producing aggregation failed, including developing cells in shaking culture in the presence of exogenous cAMP pulses. Activation of adenylyl cyclase (ACA) and actin polymerization is summarized from Fig. 4 where (+++) indicates a response indistinguishable from wild-type, (++) indicates a consistently smaller peak response and (±) indicates a reproducible but very weak activation of the enzyme. GTP inhibition of cAMP binding is presented as the percentage reduction of [^{3}H]cAMP bound to the membrane in the presence of exogenous GTP compared to the absence of added GTP. Values shown are the mean ± S.E. of triplicate determinations from two to four independent experiments performed on postaggregation (Dev.) and preaggregation (Veg.) cells. The amount of receptors in the membrane preparations was verified after binding experiments by immunoblot (data not shown).

Mutant class	Substitutions	Phenotype DB	ACA activation	Actin polymerization	GTP inhibition		Ca^{2+} influx	
					Dev.	Veg.	Ratio	*n*
Wild-type		+++	++	+++	63 ± 11	67 ± 1	4.9	3
I-21	I108N	−	−	−	4 ± 10	2.4 ± 3	1.0	3
I-22	H191P	−	±	ND[a]	1 ± 2	6 ± 6	ND	ND
II-21	R160S,H191P	−	−	−	10 ± 0	ND	1.0	3
II-22	R160S	+++	++	++	ND	ND	ND	ND
IIIa-21	N210S	+++	+++	+++	62 ± 0	ND	ND	ND
IIIa-22	I171V,Y259H	+++	ND	ND[a]	62 ± 0	ND	ND	ND
IIIb-21	N229D	+	+++	+++	ND	ND	ND	ND
IIIb-22	L107S,F164Y,N197I,I208Y	+	ND	ND[a]	ND	ND	ND	ND
IIIc-21	S90R,V189A	−	ND	ND[a]	NA[b]	NA	NA	NA
IIIc-22	T97A,V136T	−	ND	ND[a]	NA[b]	NA	NA	NA

[a] ND, not determined.
[b] NA, not applicable.

heterotrimeric G protein, this might sterically impede G protein independent signaling as well. A second possibility is that the specific residues mutated in I-21 and I-22 might serve as contact sites shared by multiple effectors, such as G proteins, and those mediating Ca^{2+} influx and activation of other G protein independent signal processes. We favor the third possibility that the catalytic G protein coupling and Ca^{2+} influx may all require the formation of a specific activated receptor conformation distinct from that recognized by the receptor kinase. Further evidence for multiple activated states is presented in a companion study (50) where signaling mutants impaired in multiple pathways as well as in a specific function are isolated and characterized. Combined with the class I mutants of this study, these observations lead us to propose that G protein-coupled receptors can undergo multiple activational isomerization steps. Upon agonist binding, the receptor first undergoes conformational changes, which allow its interaction with a receptor-specific kinase. Then it undergoes additional changes, which allow it to interact with G proteins and with factor(s) mediating G protein-independent signaling processes.

The distribution of mutants among the different functional classes was not definitively established. However, from the initial screens, it is clear that most fall into classes IIIa and IIIb, as nearly two-thirds exhibited impaired phosphorylation

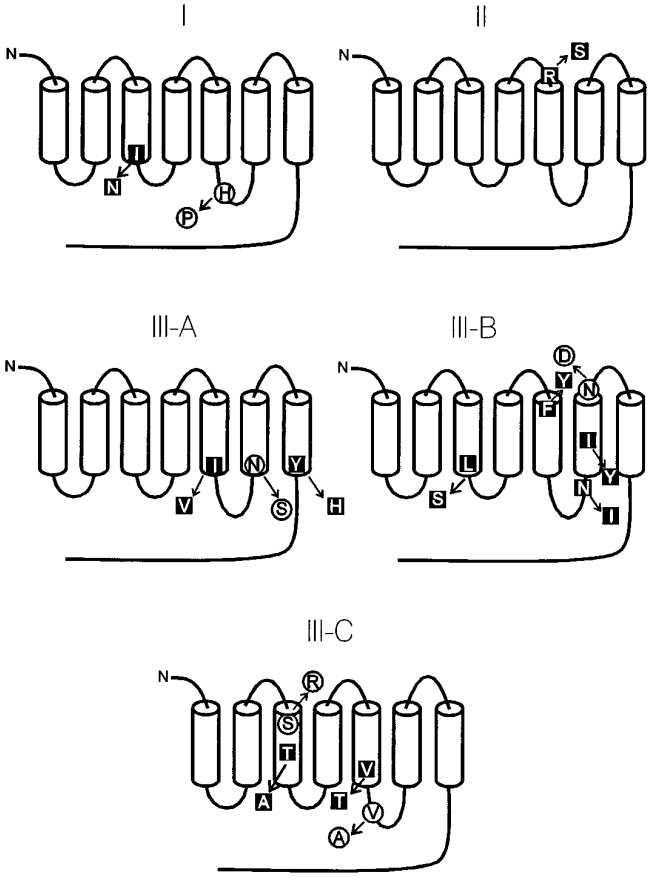

FIG. 7. **Summary of representative cAR1 mutations.** Barrels represent the proposed transmembrane domains of cAR1. Amino acid substitutions in each of the mutants are shown corresponding to their locations in this topological cAR1 model. The loops interconnecting the barrels on the *top* represents extracellular domains while the loops at the *bottom* depicts intracellular domains of the receptor. The *roman numeral* on top of each drawing indicates the class to which each of these mutants belong. The mutagenesis was carried out within the shaded region of Fig. 1. The single-letter designation of the amino acid substitutions in each mutants are indicated with the wild-type residues at the tail of the *arrow* and the mutated residue at the head. When two mutants are represented in a model of receptor, the first member of the class (*e.g.* I-21) is represented by *white letters* within *filled squares*, while the second member (*e.g.* I-22) is represented by *filled letters* inside of a *clear circle*.

at low but not high cAMP concentrations. This observation suggests that there are many more ways to selectively disrupt cAMP binding affinity than transmembrane signaling. This may reflect a relatively larger number of amino acid residues influencing ligand binding. Our observations also indicate that cAR1 can be extensively substituted and still functionally and phenotypically replace wild-type receptors. This sequence flexibility may account for the ability of GPCRs of widely different sequences to perform a similar set of biochemical functions and explain why during the course of evolution, changes in ligand binding affinity and specificity occur more readily than changes in signaling functions. Moreover, those binding alterations may occur in quantitatively discrete steps, as in the class III mutants of this study. Such modular affinity alterations could account for the polymorphisms in hormonal and pharmacological responsiveness exhibited by the human population.

Acknowledgment—We thank the Genetic Resources CORE Facility at Johns Hopkins University for sequencing the mutant cDNA sequences.

REFERENCES

1. Dohlman, H. G., Thorner, J., Caron, M. G., and Lefkowitz, R. J. (1991) *Annu. Rev. Biochem.* **60,** 653–688
2. Strader, C. D., Fong, T. M., Graziano, M. P., and Tota, M. R. (1995) *FASEB J.* **9,** 745–754
3. Fishman, H. A., Orwar, O., Scheller, R. H., and Zare, R. N. (1995) *Proc Natl. Acad. Sci. U. S. A.* **92,** 7877–7881
4. Haribabu, B., and Snyderman, R. (1993) *Proc. Natl. Acad. Sci. U. S. A.* **90,** 9398–9402
5. Misrahi, M., Vu Hai, M. T., Meduri, G., Loosfelt, H., Atger, M., Gross, B., Jolivet, A., and Milgrom, E. (1994) *Ann. Endocrinol.* **55,** 75–78
6. Strosberg, A. D., Camoin, L., Blin, N., and Maigret, B. (1993) *Drug Des. Discov.* **9,** 199–211
7. Bourne, H. R. (1989) *Nature* **337,** 504
8. Boyer, J. L., Waldo, G. L., and Harden, T. K. (1992) *J. Biol. Chem.* **267,** 25451–25456
9. Brechler, V., Reichlin, S., De Gasparo, M., and Bottari, S. P. (1994) *Receptors Channels* **2,** 89–98
10. Milne, J. L. S., Wu, L., Caterina, M. J., and Devreotes, P. N. (1995) *J. Biol. Chem.* **270,** 5926–5931
11. Caterina, M. J., Devreotes, P. N., Borleis, J., and Hereld, D. (1995) *J. Biol. Chem.* **270,** 8667–8672
12. Chen, C.-K., Inglese, J., Lefkowitz, R. J., and Hurley, J. B. (1995) *J. Biol. Chem.* **270,** 18060–18066
13. Benovic, J. L., Onorato, J. J., Caron, M. G., and Lefkowitz, R. J. (1990) *Soc. Gen. Physiol. Ser.* **45,** 87–103
14. Strader, C. D., Fong, T. M., Tota, M. R., Underwood, D., and Dixon, R. A. (1994) *Annu. Rev. Biochem.* **63,** 101–132
15. Savarese, T. M., Wang, C.-D., and Fraser, C. M. (1992) *J. Biol. Chem.* **267,** 11439–11448
16. Strader, C. D., Sigal, I. S., Candelore, M. R., Rands, E., Hill, W. S., and Dixon, R. A. F. (1988) *J. Biol. Chem.* **263,** 10267–10271
17. Strader, C. D., Sigal, I. S., and Dixon, R. A. (1989) *FASEB J.* **3,** 1825–1832
18. Strader, C. D., Sigal, I. S., and Dixon, R. A. (1989) *Am. J. Respir. Cell Mol. Biol.* **1,** 81–86
19. Kobilka, B. K., Kobilka, T. S., Daniel, K., Regan, J. W., Caron, M. G., and Lefkowitz, R. J. (1988) *Science* **240,** 1310–1316
20. Savarese, T. M., and Fraser, C. M. (1992) *Biochem. J.* **283,** 1–19
21. Bonner, J. T. (1949) *Sci. Am.* **180,** 44–47
22. Devreotes, P. N. (1994) *Neuron* **12,** 235–241
23. Wu, L., Valkema, R., Van Haastert, P. J., and Devreotes, P. N. (1995) *J. Cell Biol.* **129,** 1667–1675
24. Sun, T. J., and Devreotes, P. N. (1991) *Genes Dev.* **5,** 572–582
25. Hereld, D., Vaughan, R., Kim, J. Y., Borleis, J., and Devreotes, P. (1994) *J. Biol. Chem.* **269,** 7036–7044
26. Cadwell, R. C., and Joyce, G. F. (1992) *PCR Methods Appl.* **2,** 28–33
27. Caterina, M. J., Milne, J. L. S., and Devreotes, P. N. (1994) *J. Biol. Chem.* **269,** 1523–1532
28. Kim, J.-Y., and Devreotes, P. N. (1994) *J. Biol. Chem.* **269,** 28724–28731
29. Vaughan, R. A., and Devreotes, P. N. (1988) *J. Biol. Chem.* **263,** 14538–14543
30. Klein, P. S., Sun, T. J., Saxe, C. L., III, Kimmel, A. R., Johnson, R. L., and Devreotes, P. N. (1988) *Science* **241,** 1467–1472
31. Parent, C. A., and Devreotes, P. N. (1995) *J. Biol. Chem.* **270,** 22693–22696
32. Lilly, P. J., and Devreotes, P. N. (1994) *J. Biol. Chem.* **269,** 14123–14129
33. Condeelis, J., and Hall, A. L. (1991) *Methods Enzymol.* **196,** 486–496
34. Van Haastert, P. J. M. (1984) *Biochem. Biophys. Res. Commun.* **124,** 597–604
35. Milne, J. L., and Devreotes, P. N. (1993) *Mol. Biol. Cell* **4,** 283–292
36. Klein, P., Theibert, A., Fontana, D., and Devreotes, P. N. (1985) *J. Biol. Chem.* **260,** 1757–1764
37. Klein, P., Vaughan, R., Borleis, J., and Devreotes, P. (1987) *J. Biol. Chem.* **262,** 358–364
38. Hereld, D., and Devreotes, P. N. (1992) *Int. Rev. Cytol.* **137B,** 35–47
39. Van Haastert, P. J. M. (1985) *Biochim. Biophys. Acta* **845,** 254–260
40. Pupillo, M., Insall, R., Pitt, G. S., and Devreotes, P. N. (1992) *Mol. Biol. Cell* **3,** 1229–1234
41. Insall, R. H., Soede, R. D., Schaap, P., and Devreotes, P. N. (1994) *Mol. Biol. Cell* **5,** 703–711
42. Johnson, R. L., Van Haastert, P. J. M., Kimmel, A. R., Saxe, C. L., III, Jastorff, B., and Devreotes, P. N. (1992) *J. Biol. Chem.* **267,** 4600–4607
43. Saxe, C. L., III, Ginsburg, G. T., Louis, J. M., Johnson, R., Devreotes, P. N., and Kimmel, A. R. (1993) *Genes Dev.* **7,** 262–272
44. Wu, L. J., Valkema, R., Van Haastert, P. J. M., and Devreotes, P. N. (1995) *J. Cell Biol.* **129,** 1667–1675
45. Van Haastert, P. J. M., De Vries, M. J., Penning, L. C., Roovers, F., Van Der Kaay, J., Erneux, C., and Van Lookeren Campagne, M. M. (1989) *Biochem. J.* **258,** 577–586
46. Kim, J.-Y., Van Hasstert, P. J. M., and Devreotes, P. N. (1996) *Chem. Biol.* **3,** 239–243
47. Weiner, J. L., Guttierez-Steil, C., and Blumer, K. J. (1993) *J. Biol. Chem.* **268,** 8070–8077
48. Saxe, C. L., III, Johnson, R., Devreotes, P. N., and Kimmel, A. R. (1991) *Dev. Genet.* **12,** 6–13
49. Franke, R. R., Konig, B., Sakmar, T. P., Khorana, H. G., and Hofmann, K. P. (1990) *Science* **250,** 123–125
50. Milne, J. L. S., Caterina, M. J., and Devreotes, P. N. (1997) *J. Biol. Chem.* **272,** 2069–2076